JOURNAL OF GUIDANCE, CONTROL, AND DYNAMICS
Vol. 24, No. 1, January–February 2001

Lyapunov Control Law for Slew Maneuver Using Time Finite Element Analysis

Jinyoung Suk* and Sunwoong Boo†
Korea Aerospace Industries, Ltd., Changwon 641-600, Republic of Korea
and
Youdan Kim‡
Seoul National University, Seoul 151-742, Republic of Korea

The Lyapunov control law for the slew maneuver of flexible space structure is designed using a time-domain finite element analysis. Closed-loop dynamics of the hybrid system is analyzed, expanding the results of open-loop dynamics on the spatial propagation of the appendage. Lagrange multipliers are included to guarantee the rest-to-rest maneuver, and the resulting dynamics are solved in the optimization perspective. As a result, the motion of the rigid/flexible modes is governed by the feedback gains. An efficient parameter optimization method is suggested in combination with the time-domain finite element analysis. It serves a concurrent general optimization algorithm that is applicable to partial-state feedback systems. To optimize the gain set of the control system, an energy-based performance index is adopted, and the gradients of the performance index with respect to each gain are derived. Several numerical results are shown to demonstrate the result of the integrated modeling–optimization scheme.

I. Introduction

HAMILTON'S law has been a key approach in analyzing dynamic systems. Application of Hamilton's law in dynamics has become a classical alternative in the computer age. Combined with Bailey's[1,2] reinvestigation of Hamilton's law, the time-domain finite element method is proposed as a new approach to analytical dynamics.[1–6] With the development of time-domain finite element analysis, alternative methods were found for optimization problems without resorting to the conventional optimization algorithms. Hodges and Bless,[7] Bless et al.,[8] Hodges et al.,[9] and Lee and Kim[10] are notable works using variations of the performance index and time-finite element discretization. Öz and Adiguzel suggested a way to generalize the quadratic performance index in time-domain finite element analysis.[11] However, there exists a problem in the computational efficiency of the time finite element analysis. The computational efficiency depends on how complicated the selected model is and how accurate the analysis will be. From the simple (but effective) model to a very complicated system, to be capable of real-time implementation a huge amount of memory and hours of computational time are required even though the computational burden can be greatly reduced using the sparsity characteristics of the constructed matrices. In particular, when the distributed parameter system is solved by using the time finite element analysis, too much processing time is required, which depends on the number of both time- and space-discrezied finite elements. Our motivation is to reduce the computational burden in analyzing the distributed parameter system, for example, flexible space structures, using time finite element analysis.

Modern optimal control theory allows effective feedback systems using the full state and/or output feedback control methodology.[12–14] The theory offers a unique solution corresponding to a certain control objective with the boundary conditions imposed on the state-costate pair. It has been applied to almost all kinds of optimization problems that may be formulated in state space. From the optimization perspective, however, it is difficult to maximize the feedback effect of some specified states. This could happen in the gain optimization of the Lyapunov feedback controller because the variables used in the feedback routine are usually a subset of the states. Unfortunately, it is very hard to systemize the procedure for this kind of feedback system. In this case, there would be an optimization algorithm based on the eigensystem analysis in the time domain to get a closed-form performance index that, in general, is expressed as a lot of transcendental terms.[15,16] The ensuing nonlinear dynamic programming requires a lot of time, and the results are usually sensitive to the initial condition, irrespective of the applied optimization technique. Also, it is important to calculate the gradient of the performance index with respect to each parameter in the nonlinear optimization algorithm, and an efficient optimization procedure would require a simple and general form of the expression of gradients. On the other hand, there are many interesting research works on the optimal slewing of the flexible space structures, only a few of them are referenced here.[17–19] All of these references were focused on precision targeting with a great effort to minimize the vibration during the slew maneuver. In particular, Singhose et al. propose a robust and simple control algorithm using input shaping.[19]

This paper presents a modeling method of the closed-loop system to slew flexible space structures using time finite element analysis. Two types of control laws are used to achieve the mission objectives: the constant gain feedback control law and the tracking control law to follow the reference maneuver. Both control laws are designed based on Lyapunov's stability theorem. In open-loop dynamics, the spatial distribution of the slew angle history can be solved by using a matrix algebraic equation.[20] Unlike the open-loop system, closed-loop dynamics requires an explicit formulation of the constraint equations. To facilitate this, Lagrange multipliers are introduced and the dynamic equations are augmented so that the whole system may be solved from the optimization perspective. As a result, the slew angle can be expressed as a function of the selected gain set. Time-domain discretization is conducted based on Galerkin's weak formulation for the case in which the initial displacement and the final momentum of the system are specified.[21] A generalization of the suggested modeling method shows an advantage: a time-based model reduction that enables a drastic reduction of the size of the model.

This paper also suggests a method for the parameter optimization of feedback control systems for the slew maneuver of flexible space structures. The proposed method is the conventional optimization theory combined with time finite element modeling. It provides a general optimization procedure because it uses a time finite element discretization of the energy-based performance index combined with the equation of motion also derived by time finite element analysis. Therefore, an efficient optimization is obtained with simple formulations of the performance index and its gradients. The

Received 1 December 1998; revision received 10 May 2000; accepted for publication 10 May 2000.

*Research Engineer, Aerospace Research Center. Member AIAA.
†Research Engineer, Aerospace Research Center.
‡Associate Professor, Department of Aerospace Engineering, Institute of Advanced Machinery and Design. Senior Member AIAA.

method is also applicable to the optimization of partial-state feedback gains. Several numerical results are demonstrated to verify the proposed dynamics/optimization procedure using the time finite element analysis.

II. Equations of Motion

In this section, the dynamics of the closed-loop slewing flexible structure is investigated. Consider a single-axis planar rotational maneuver of a flexible space structure with a central hub and four appendages. The hybrid system of ordinary and partial differential equations governing the dynamics of this system are[22]

$$\rho\ddot{w}(x,t) + \rho x\ddot{\theta} + \frac{\partial^2}{\partial x^2}\left\{EI\frac{\partial^2 w(x,t)}{\partial x^2}\right\} = 0 \tag{1}$$

$$J_h\ddot{\theta} + 4\int_r^l \rho x[\ddot{w}(x,t) + x\ddot{\theta}]\,\mathrm{d}x = u_r(t) \tag{2}$$

where x is a spatial variable measured from the outer radius of the hub along the undeformed appendage axis, $\theta(t)$ is the slew angle, and $w(x,t)$ is the transverse deflection of the appendage measured from the x axis. Also, r is the radius of the hub, J_h is the moment of inertia of the hub, L is the length of the appendage, $l = r + L$, and $u_r(t)$ is the external torque generated by the reaction wheel mounted on the central hub. We make an assumption that the flexible appendage is a Euler–Bernoulli beam that has negligible shear/axial deformation. Furthermore, the slew motion of the flexible space is assumed slow enough to neglect the centrifugal stiffening effect. To apply the Galerkin approximation, we used the weighting function that is equivalent to taking the variation in Hamilton's weak principle. After multiplying Eq. (1) by the weighting function v and integrating over the finite time, we obtain

$$\int_{t_0}^{t_f}\rho\ddot{w}\,v\,\mathrm{d}t + \int_{t_0}^{t_f}\rho x\ddot{\theta}\,v\,\mathrm{d}t + \int_{t_0}^{t_f} EIw^{(4)}v\,\mathrm{d}t = 0 \tag{3}$$

The first two terms are rearranged using the integration by parts, where the following rest-to-rest assumption is used:

$$\dot{w}(x,t_0) = 0, \qquad \dot{w}(x,t_f) = 0, \qquad \dot{\theta}(t_0) = 0, \qquad \dot{\theta}(t_f) = 0 \tag{4}$$

$$-\int_{t_0}^{t_f}\rho\dot{w}\,\dot{v}\,\mathrm{d}t - \int_{t_0}^{t_f}\rho x\dot{\theta}\dot{v}\,\mathrm{d}t + \int_{t_0}^{t_f} EIw^{(4)}v\,\mathrm{d}t = 0 \tag{5}$$

Let us apply the time finite element method to Eq. (5). The rigid-body and flexible coordinates are discretized using the shape functions $\phi_i(t)$ such that

$$w(x,t) = \sum_j \phi_j(t)w_j(x), \qquad v(x,t) = \sum_j \phi_j(t)v_j(x)$$

$$\theta(t) = \sum_i \phi_i(t)\theta_i \tag{6}$$

Note that it can be readily known from Eq. (5) that the selected shape functions are C^1 continuous. Also, $w_j(x)$ has scalar value in time but is still a variable in the space domain. This means we have a spatial degree of freedom to be worked out. By the arrangement of the terms related to v_j, the following matrix ordinary differential equation is obtained for the structural mode:

$$-M\boldsymbol{w}(x) - M\boldsymbol{\theta}x + K\boldsymbol{w}^{(4)}(x) = 0 \tag{7}$$

where

$$M_{ij} = \int_{\Delta t}\rho\dot{\phi}_i(t)\dot{\phi}_j(t)\,\mathrm{d}t, \qquad K_{ij} = \int_{\Delta t} EI\phi_i(t)\phi_j(t)\,\mathrm{d}t$$

where

$$\int_{\Delta t}(\,)\,\mathrm{d}t$$

is the integration over the ith time finite element. The standard finite element assembly procedures are applied using initial and terminal (rest-to-rest) conditions. The boundary conditions applied are in mixed form using the Dirichlet and Neumann boundary conditions. It is not always possible to convert the Neumann boundary condition into a mixed form because a certain compatibility condition should be satisfied. The dynamic system's equivalence of this compatibility condition (conservation of the equivalent flux) is the momentum conservation principle. The compatibility condition is satisfied because the dynamic system always preserves the equivalent linear and angular momentum in the sense that the rate of the linear and angular momentum reflects on the sum of the equivalent external force and moment.

The matrix equation for the slew mode can be obtained by a similar approach. Multiplying Eq. (2) by the weighting function ϑ and integrating by parts with the initial and final conditions, we have

$$-\int_{t_0}^{t_f} J_h\dot{\theta}\dot{\vartheta}\,\mathrm{d}t - 4\int_{t_0}^{t_f}\int_r^l \rho x(\dot{w} + x\dot{\theta})\,\mathrm{d}x\,\vartheta\,\mathrm{d}t = \int_{t_0}^{t_f} u_r(t)\vartheta\,\mathrm{d}t \tag{8}$$

After finite element discretization of Eq. (8) using

$$\vartheta(t) = \sum_i \phi_i(t)\vartheta_i$$

and arranging the terms related to ϑ_j, we obtain the following matrix ordinary differential equation for the slew mode:

$$-\frac{J_{\mathrm{tot}}}{\rho}M\theta - 4M\int_r^l xw(x)\,\mathrm{d}x = \boldsymbol{F}_0 \tag{9}$$

where $J_{\mathrm{tot}} = J_h + 4\rho(l^3 - r^3)/3$ and the ith element of the vector $\boldsymbol{F}_0$ is

$$\int_{\Delta t} u_r(t)\phi_i(t)\,\mathrm{d}t$$

Equation (9) shows that the slew mode is activated by the external moment and coupled with the flexible mode. Now, the time finite element method is used to derive a matrix model that has a variable in space. The modeled flexible space structure has some spatial characteristics. Freezing the time axis and allowing freedom in the spatial axis have some positive features. Insight is provided on how the various structural properties, that is, transverse deflection, transverse angle, and moment and shear, propagate throughout the structure. Furthermore, the spatial distribution of the actuator force/moment along the structure can be designed utilizing the degree of freedom in the spatial domain. The slew motion, however, is only expressed in time, leaving no extra variables. It is wholly dependent on time. This vector is affected by how the hub control torque acts and how severe the coupling effect is between slew and flexible modes.

Now, consider the following generalized eigenvalue problem of mass matrix and stiffness matrix in Eq. (7):

$$MP = KP\Lambda \tag{10}$$

where Λ is the diagonal matrix composed of the generalized eigenvalues and P is the modal matrix consisting of the generalized eigenvectors. Note that the column vectors of P form a basis that describes the time response of the flexible appendage. Let us introduce the modal coordinate transformation

$$\boldsymbol{w}(x) = P_\eta\boldsymbol{\eta}(x) \tag{11}$$

where P_η and P_ξ are the modal matrices that retain a specified number of eigenvectors, starting from the lowest mode, and the following normalization equations are used:

$$P_\eta^T K P_\eta = I_\eta, \qquad P_\eta^T M P_\eta = \Lambda_\eta$$

Using modal coordinate transformation, we obtain the reduced-order model as follows:

$$\boldsymbol{\eta}^{(4)}(x) = \Lambda_\eta \boldsymbol{\eta}(x) + P_\eta^T M \boldsymbol{\theta} x \tag{12}$$

$$-\frac{J_{\text{tot}}}{\rho} M\boldsymbol{\theta} - 4MP_\eta \left\{ \int_r^l x\boldsymbol{\eta}(x)\,\mathrm{d}x \right\} = \boldsymbol{F}_0 \tag{13}$$

The fourth-order differential equation (12) can be transformed into the first-order system

$$\boldsymbol{y}' = A\boldsymbol{y} + Bx \tag{14}$$

where

$$A = \begin{bmatrix} 0 & \boldsymbol{I} & 0 & 0 \\ 0 & 0 & \boldsymbol{I} & 0 \\ 0 & 0 & 0 & \boldsymbol{I} \\ \Lambda_\eta & 0 & 0 & 0 \end{bmatrix}, \qquad B(\boldsymbol{\theta}) = \begin{bmatrix} 0 \\ 0 \\ 0 \\ P_\eta^T M\boldsymbol{\theta} \end{bmatrix}, \qquad \boldsymbol{y} = \begin{bmatrix} \boldsymbol{\eta} \\ \boldsymbol{\eta}' \\ \boldsymbol{\eta}'' \\ \boldsymbol{\eta}''' \end{bmatrix}$$

Augmented state vectors represent the time trajectories of transverse deflection, transverse angle, mechanical moment, and shear force, respectively. The response of the flexible appendage at an arbitrary point can be obtained as follows:

$$\boldsymbol{y}(x) = e^{A(x-r)}\boldsymbol{y}(r) + \int_r^x e^{A(x-\zeta)} B\zeta\,\mathrm{d}\zeta, \qquad r \le x \le l$$

$$= e^{A(x-r)}\boldsymbol{y}(r) + \boldsymbol{\Phi}\Sigma(x)\boldsymbol{\Phi}^{-1}B(\boldsymbol{\theta}) \tag{15}$$

where $\boldsymbol{\Phi}$ is the modal matrix of A, and if λ_i is the ith eigenvalue of A, then

$$\Sigma(x) = \mathrm{diag}\{\ldots, \sigma_i(x), \ldots\}$$

$$\sigma_i(x) = e^{\lambda_i(x-r)}\left\{r/\lambda_i + 1 | \lambda_i^2\right\} - \left\{x/\lambda_i + 1 | \lambda_i^2\right\}$$

are the integration of the second term in Eq. (15). Equation (15) shows that the time trajectory of the structural mode consists of two terms: 1) the spatially propagated mechanical properties originated from the root of the appendage and 2) the effect of the hub control torque combined with peculiar eigenstructure characteristics of the flexible structure system. Now, the motion of the tip of the flexible appendage can be obtained as follows:

$$\boldsymbol{y}(l) = e^{AL}\boldsymbol{y}(r) + \boldsymbol{\Phi}\Sigma(l)\boldsymbol{\Phi}^{-1}B(\boldsymbol{\theta})$$

$$\equiv \boldsymbol{\Omega}\boldsymbol{y}(r) + \boldsymbol{\Psi}B(\boldsymbol{\theta}) \equiv \boldsymbol{\Omega}\boldsymbol{y}(r) + \mu(\boldsymbol{\theta}) \tag{16}$$

Let us define new partitioned state vectors

$$\boldsymbol{y}_1(x) = \begin{pmatrix} \boldsymbol{\eta}(x) \\ \boldsymbol{\eta}'(x) \end{pmatrix}, \qquad \boldsymbol{y}_2 = \begin{pmatrix} \boldsymbol{\eta}''(x) \\ \boldsymbol{\eta}'''(x) \end{pmatrix}$$

By the use of these state vectors, Eq. (16) can be rewritten as

$$\begin{pmatrix} \boldsymbol{y}_1(l) \\ \boldsymbol{y}_2(l) \end{pmatrix} = \begin{pmatrix} \Omega_{11} & \Omega_{12} \\ \Omega_{21} & \Omega_{22} \end{pmatrix} \begin{pmatrix} \boldsymbol{y}_1(r) \\ \boldsymbol{y}_2(r) \end{pmatrix} + \begin{pmatrix} \mu_1(\boldsymbol{\theta}) \\ \mu_2(\boldsymbol{\theta}) \end{pmatrix} \tag{17}$$

With fixed–free boundary conditions of the appendage, that is, fixed at $x = r$ and free at $x = l$, which is expressed as

$$w(r,t) = 0, \qquad \left.\frac{\partial w(x,t)}{\partial x}\right|_{x=r} = 0$$

$$\left.\frac{\partial^2 w(x,t)}{\partial x^2}\right|_{x=l} = 0, \qquad \left.\frac{\partial^3 w(x,t)}{\partial x^3}\right|_{x=l} = 0$$

therefore, we have

$$\boldsymbol{y}_2(r) = -\Omega_{22}^{-1}\mu_2(\boldsymbol{\theta}) \tag{18}$$

$$\boldsymbol{y}_1(l) = \Omega_{12}\boldsymbol{y}_2(r) + \mu_1(\boldsymbol{\theta}) \tag{19}$$

Note that in Eqs. (18) and (19), all of the state vectors are represented as a function of $\boldsymbol{\theta}$. The information of vector $\boldsymbol{\theta}$ can be obtained by Eq. (13). Then, the spatial distribution of the mechanical characteristics of the slewing appendages can be determined by Eq. (15). To obtain the solution of Eq. (13), the integration

$$\int_r^l x\boldsymbol{\eta}(x)\,\mathrm{d}x$$

should first be transformed into a function of $\boldsymbol{\theta}$. The following equation can be obtained by using Eq. (15):

$$\int_r^l x\boldsymbol{y}(x)\,\mathrm{d}x = \int_r^l e^{A(x-r)}x\boldsymbol{y}(r)\,\mathrm{d}x + \int_r^l \boldsymbol{\Phi}\Sigma(x)\boldsymbol{\Phi}^{-1}B(\boldsymbol{\theta})x\,\mathrm{d}x$$

$$\equiv \boldsymbol{\Phi\Theta\Phi}^{-1}\boldsymbol{y}(r) + \boldsymbol{\Phi\Xi\Phi}^{-1}B(\boldsymbol{\theta}) \tag{20}$$

where $\boldsymbol{\Theta}$ and $\boldsymbol{\Xi}$ are the diagonal matrices, respectively, whose diagonal terms are represented as follows:

$$\boldsymbol{\Theta}_{ii} = e^{\lambda_i L}\left\{l/\lambda_i - 1 | \lambda_i^2\right\} - \left\{r/\lambda_i - 1 | \lambda_i^2\right\}$$

$$\boldsymbol{\Xi}_{ii} = -\left[(l^3 - r^3) | 3\lambda_i + (l^2 - r^2) | 2\lambda_i^2\right] + \left\{r/\lambda_i + 1 | \lambda_i^2\right\}$$
$$\times \left\{e^{\lambda_i L}\left(l/\lambda_i - 1 | \lambda_i^2\right) - \left(r/\lambda_i - 1 | \lambda_i^2\right)\right\}$$

Therefore, by substitution of Eq. (18) into Eq. (20),

$$\int_r^l x\boldsymbol{\eta}(x)\,\mathrm{d}x$$

can be obtained as

$$\int_r^l x\boldsymbol{\eta}(x)\,\mathrm{d}x = \left\{\Pi_{11,44} - \Gamma_{11,34}\Omega_{22}^{-1}\Psi_{34,44}\right\}P_\eta^T M\boldsymbol{\theta} \tag{21}$$

where $\Pi = \Phi\Xi\Phi^{-1}$ and $\Gamma = \Phi\Theta\Phi^{-1}$ and matrices $\Pi_{ij,kl}$, $\Gamma_{ij,kl}$, and $\Psi_{ij,kl}$ are submatrices consisting of ij rows and kl columns of Π, Γ, and Ψ, respectively, when the individual matrix is divided into 4×4 square submatrices. For example, $\Gamma_{11,34}$ means the submatrix of Γ, which has the first row and third/fourth column when Γ is divided into 4×4 square submatrices.

Using Eq. (13) and Eq. (21), we obtain the following equation:

$$\boldsymbol{\theta} = -\left[(J_{\text{tot}}/\rho)M + 4MP_\eta\left\{\Pi_{11,44} - \Gamma_{11,34}\Omega_{22}^{-1}\Psi_{34,44}\right\}P_\eta^T M\right]^{-1}\boldsymbol{F}_0 \tag{22}$$

For a given control input $u_r(t)$, the time response of the slew mode can be solved explicitly from Eq. (22), and the motion of the flexible appendage can be obtained from Eqs. (14) and (11) with initial conditions.

III. Slew Maneuver of Feedback Control System

In this section, the rest-to-rest maneuver of a feedback control system is studied using time-domain finite element analysis. The model reduction scheme in time-based modal coordinates can also be applied to a closed-loop system analogous to an open-loop system. Two types of control laws are used to develop the time-domain finite element version for the closed-loop slew maneuver. One is the constant gain feedback control law[22,23] and the other is a tracking control law based on the optimal torque shaping via a Fourier series expansion.[24] Both control laws are designed based on the Lyapunov stability theory.

Constant Gain Feedback Control Law

There has been much research on the effective control methodology for both slewing and vibration control. It is known that the global stability of the Lyapunov controller is guaranteed irrespective of the selected gain set when the Lyapunov candidate function is positive semidefinite and its first time derivative is negative semidefinite. The first control law is developed by taking a summation of 1) the kinetic energy, 2) the potential energy, and 3) the error energy between the target angle and the temporal state for the slew mode, as a Lyapunov function:

$$U = a_1\frac{1}{2}J_h\dot{\theta}^2 + a_2\frac{1}{2}(\theta-\theta_f)^2 + 4a_3\left\{\frac{1}{2}\int_r^l \rho(\dot{w}+x\dot{\theta})^2\,\mathrm{d}x + \frac{1}{2}\int_r^l \rho\left(\frac{\partial^2 w}{\partial x^2}\right)^2\mathrm{d}x\right\} \tag{23}$$

Note that the global minimum of $U = 0$ occurs only at the desired state. A constant gain feedback control law is derived from Eq. (23); a detailed derivation of the control law can be found in Ref. 22:

$$u_r(t) = -g_1\{\theta(t)-\theta_f\} - g_2\dot{\theta}(t) - g_3\left\{\int_r^l \rho x\ddot{w}(x,t)\,\mathrm{d}x + \int_r^l \rho x^2\ddot{\theta}(t)\,\mathrm{d}x\right\} \tag{24}$$

where θ_f is the target angle and g_i are the gains to enhance the slew performance. Gains are to be chosen to guarantee the stability of the closed-loop system such that $g_1 > 0$, $g_2 > 0$, and $g_3 > -4$. These constraints render the time derivative of the Lyapunov candidate function negative semidefinite. The last term of the Lyapunov control law, related to the second time derivatives of hub rotation and spatial displacement, is summarized as a shear and moment applied to the root of an appendage and can be expressed as follows:

$$-(M_0 - S_0 l_0) = \int_r^l \rho(\ddot{w}+x\ddot{\theta})\,\mathrm{d}x \tag{25}$$

In view of the real implementation, strain sensors are used instead of using the acceleration. It can be derived readily that the root moment and shear is transferred to the strain at the root of the appendage. Therefore, the root shear and bending moment can be measured by conventional strain gauges or piezoelectric sensors. Strain gauges are used by Junkins et al.,[22] and piezoelectric sensors are used by Suk et al.[25] Both experiments show successful results for slew maneuver and vibration suppression.

By substitution of Eq. (24) into Eq. (2), the slew maneuver of the closed-loop system is obtained as

$$\left[J_{\text{tot}} + g_3\int_r^l \rho x^2\,\mathrm{d}x\right]\ddot{\theta}(t) + g_2\dot{\theta}(t) + g_1\theta(t) + (g_3+4)\int_r^l \rho x\ddot{w}(x,t)\,\mathrm{d}x = g_1\theta_f \tag{26}$$

Multiplying Eq. (26) by ϑ and integrating over the time give

$$\int_{t_0}^{t_f}\left\{\left[J_{\text{tot}} + g_3\int_r^l \rho x^2\,\mathrm{d}x\right]\ddot{\theta}(t) + g_2\dot{\theta}(t) + g_1\theta(t) + (g_3+4)\int_r^l \rho x\ddot{w}(x,t)\,\mathrm{d}x\right\}\vartheta\,\mathrm{d}t = \int_{t_0}^{t_f} g_1\theta_f\vartheta\,\mathrm{d}t \tag{27}$$

After discretizing the preceding equation, we obtain

$$\frac{-J_{\text{tot}} + g_3[\rho(l^3-r^3)/3]}{\rho}\boldsymbol{M\theta} + g_2\boldsymbol{C\theta} + \frac{g_1}{EI}\boldsymbol{K\theta} - (g_3+4)\boldsymbol{M}\int_r^l x\boldsymbol{w}(x)\,\mathrm{d}x = \boldsymbol{F}(g_1) \tag{28}$$

where

$$C_{ij} = \int_{\Delta t}\phi_i(t)\dot{\phi}_j(t)\,\mathrm{d}t, \qquad F_i(g_1) = \int_{\Delta t} g_1\theta_f\phi_i(t)\,\mathrm{d}t$$

Note that matrix C is skew symmetric. It is impossible to perform model reduction in the rigid mode due to the existence of the slew rate feedback. On the contrary, the root moment feedback in the flexible mode emancipates this restriction, which enables the manipulation of the spatial propagation with a small number of structural time modes. By use of Eq. (28) and some mathematical operations, the slewing motion of the closed-loop system can be expressed as a function of the feedback gains as follows:

$$\boldsymbol{\theta}(g_1,g_2,g_3) = \Big(-\big\{J_{\text{tot}} + g_3[\rho(l^3-r^3)/3]\big\}(M/\rho) + g_2C + (g_1/EI)K + (g_3+4)MP_\eta \times\big(\Pi_{11,44} - \Gamma_{11,34}\Omega_{22}^{-1}\Psi_{34,44}\big)P_\eta^T M\Big)^{-1}\boldsymbol{F}(g_1) \tag{29}$$

Tracking Control Law

The second control law is designed to follow the reference maneuver utilizing the Lyapunov stability theorem. To obtain the tracking control law, the optimal torque shaping maneuver is selected as a reference trajectory.[24] The following tracking control law can be obtained from the candidate tracking error energy Lyapunov function:

$$u_r(t) = u_{\text{ref}}(t) - g_1\{\theta(t)-\theta_{\text{ref}}(t)\} - g_2\{\dot{\theta}(t)-\dot{\theta}_{\text{ref}}(t)\} - g_3\left\{\int_r^l \rho x\ddot{w}(x,t)\,\mathrm{d}x + \int_r^l \rho x^2\ddot{\theta}(t)\,\mathrm{d}x - \int_r^l \rho x^2\,\mathrm{d}x\ddot{\theta}_{\text{ref}}(t)\right\} \tag{30}$$

where

$$u_{\text{ref}}(t) = \sum_j a_j\sin\frac{2\pi jt}{t_f}$$

and $\theta_{\text{ref}}(t)$ and $\dot{\theta}_{\text{ref}}(t)$ are the reference slew angle and angular velocity of the central hub, respectively, when the reference torque $u_{\text{ref}}(t)$ is enforced on the rigid structure. The slewing motion of the closed-loop system becomes

$$\left[J_{\text{tot}} + g_3\int_r^l \rho x^2\,\mathrm{d}x\right]\ddot{\theta}(t) + g_2\dot{\theta}(t) + g_1\theta(t) + (g_3+4)\int_r^l \rho x\ddot{w}(x,t)\,\mathrm{d}x = u_{\text{ext}}(t) \tag{31}$$

where

$$u_{\text{ext}}(t) = u_{\text{ref}}(t) + g_1\theta_{\text{ref}}(t) + g_2\dot{\theta}_{\text{ref}}(t) + g_3\int_r^l \rho x^2\,\mathrm{d}x\ddot{\theta}_{\text{ref}}(t)$$

Following a similar procedure derived for the constant gain feedback control law, we can deduce the time history of the slew angle as a function of the gain set:

$$\boldsymbol{\theta}(g_1,g_2,g_3) = \Big(-\big\{J_{\text{tot}} + g_3[\rho(l^3-r^3)/3]\big\}(M/\rho) + g_2C + (g_1/EI)K + (g_3+4)MP_\eta\big(\Pi_{11,44} - \Gamma_{11,34}\Omega_{22}^{-1}\Psi_{34,44}\big)P_\eta^T M\Big)^{-1}F_{\text{ext}}(g_1,g_2,g_3) \tag{32}$$

where F_{ext} comes from the time finite element discretization of the external input u_{ext}.

Constraint Equations

To complete the dynamic analyses, the matrix algebraic equations (29) and (32) should be transformed into an optimization problem with the constraints described hereafter. General optimal control problems are composed of the performance index and various constraint equations such as equality/inequality constraints for both the state and input. In this study, the equality constraints are dealt with in the optimization of the feedback gains using time-domain finite element analysis. Lagrange multipliers are introduced to include the effect of additional constraints in the performance index. As a consequence, the resulting constraint equations are merged into the augmented performance index. The following constraints are imposed to perform the rest-to-rest maneuver:

$$\theta(t_0) = 0, \qquad \dot{\theta}(t_0) = 0, \qquad \theta(t_f) = \theta_f, \qquad \dot{\theta}(t_f) = 0 \tag{33}$$

where the final velocity and initial displacement for each mode have already been imposed during the time-domain finite element formulation. Thus, the following configurations are to be included in the performance index: 1) the initial slew velocity and 2) the initial velocity of the appendage.

The constraints for the initial velocity for the slew mode can be expressed as an algebraic form for a variable vector using the finite element discretization as follows:

$$\boldsymbol{\alpha}^T\boldsymbol{\theta} = 0, \qquad \boldsymbol{\alpha} = [\dot{\phi}_2(t_0), \ldots, \dot{\phi}_n(t_0), 0, \ldots, 0]^T \tag{34}$$

Note that the first shape function vanishes in deriving $\boldsymbol{\alpha}$ due to the initial displacement condition. Similarly, the constraints on the initial velocity for the flexible mode can be expressed as

$$\boldsymbol{\gamma}^T T_{\theta y}\boldsymbol{\theta} = 0, \qquad \boldsymbol{\gamma} = \begin{bmatrix} 0 & P_\eta^T \end{bmatrix} \begin{pmatrix} 0 \\ \alpha \end{pmatrix} \tag{35}$$

where

$$T_{\theta y} = \left\{ \Psi_{12} - \Omega_{12}\Omega_{22}^{-1}\Psi_{22} \right\} \begin{pmatrix} \mathbf{0} \\ P_\eta^T M \end{pmatrix} \tag{36}$$

Using Eq. (29), the slew trajectory can be rewritten as a function of the control gains

$$T_0(g_1, g_2, g_3)\boldsymbol{\theta} = g_1 F_r \tag{37}$$

where

$$T_0 = -\frac{\left\{J_{\text{tot}} + g_3[\rho(l^3 - r^3)/3]\right\}}{\rho} M + g_2 C + \frac{g_1}{EI} K + (g_3 + 4) M P_\eta \left(\Pi_{11,44} - \Gamma_{11,34}\Omega_{22}^{-1}\Psi_{34,44}\right) P_\eta^T M$$

$$[F_r]_i = \theta_f \int_{\Delta t} \phi_i \,\mathrm{d}t$$

Now, the solution for the slew mode is to be revised to accommodate the constraint equations (34) and (35). For that purpose, Eq. (36) is augmented in the optimization aspect so that the solution can be found by

$$\text{minimize} \| T_0(g_1, g_2, g_3)\boldsymbol{\theta} - g_1 F_r \| \tag{38}$$

subject to

$$\boldsymbol{\alpha}^T\boldsymbol{\theta} = 0, \qquad \boldsymbol{\gamma}^T T_{\theta y}\boldsymbol{\theta} = 0 \tag{39}$$

The augmented performance index can be defined by using the Lagrange multipliers κ_i as follows:

$$J_a = (T_0\boldsymbol{\theta} - g_1 F_r)^T (T_0\boldsymbol{\theta} - g_1 F_r) + \kappa_1 \boldsymbol{\alpha}^T\boldsymbol{\theta} + \kappa_2 \boldsymbol{\gamma}^T T_{\theta y}\boldsymbol{\theta} \tag{40}$$

We can find the closed-loop slew response using the differentiation of the performance index with respect to $\boldsymbol{\theta}$ along with the constraint equations. The resulting equations also yield the matrix algebraic form

$$\frac{\mathrm{d}J_a}{\mathrm{d}\boldsymbol{\theta}} = 0 = 2T_0^T T_0\boldsymbol{\theta} - 2g_1 T_0^T F_r + \boldsymbol{\alpha}\kappa_1 + T_{\theta y}^T\boldsymbol{\gamma}\kappa_2 \tag{41}$$

$$\frac{\mathrm{d}J_a}{\mathrm{d}\kappa_1} = 0 = \boldsymbol{\alpha}^T\boldsymbol{\theta} \tag{42}$$

$$\frac{\mathrm{d}J_a}{\mathrm{d}\kappa_2} = 0 = \boldsymbol{\gamma}^T T_{\theta y}\boldsymbol{\theta} \tag{43}$$

By the use of Eqs. (41–43), $[\boldsymbol{\theta}^T \quad \kappa_1 \quad \kappa_2]^T$ can be obtained as follows:

$$\boldsymbol{\theta}_a = \begin{bmatrix} \boldsymbol{\theta} \\ \kappa_1 \\ \kappa_2 \end{bmatrix} = T_a^{-1} \begin{bmatrix} 2T_0^T g_1 F_r \\ 0 \\ 0 \end{bmatrix} \tag{44}$$

where

$$T_a = \begin{bmatrix} 2T_0^T T_0 & \boldsymbol{\alpha} & T_{\theta y}^T\boldsymbol{\gamma} \\ \boldsymbol{\alpha}^T & 0 & 0 \\ \boldsymbol{\gamma}^T T_{\theta y} & 0 & 0 \end{bmatrix}$$

Therefore, the slew history $\boldsymbol{\theta}$ can be obtained from the augmented vector $\boldsymbol{\theta}_a$.

IV. Gain Optimization for Closed-Loop Slew Maneuver

In this section, a systematic way of obtaining the optimal feedback gains is investigated for the constant gain feedback control law. The proposed approach provides a general optimization procedure using time finite element analysis because it uses the time finite element discretization of the energy-based performance index combined with the equation of motion also derived by time finite element analysis. This kind of performance index is natural for dynamic systems in that the minimization of the kinetic energy reflects the suppression of the excitation throughout the movement of the system. In addition, the minimization of the error energy reflects the slew motion aims at precision targeting because the error energy has its minimum at the final target angle. The proposed optimization procedure has an advantage over the nonlinear dynamic programming because the solution can be extracted from a simple matrix operation. A well-designed performance index is constructed with the two objective functions using the time-domain finite element analysis. The performance index is minimized using the gradient information.

An appropriate performance index can be defined to achieve accurate targeting while minimizing the vibration energy during the maneuver. The performance index consists of two objective functions: 1) the slewing error energy against the reference target angle and 2) the vibration energy of the system during the maneuver. The first objective function can be expressed as follows:

$$J_1 = q_\theta \int_{t_0}^{t_f} [\theta(t) - \theta_f]^2 \,\mathrm{d}t \tag{45}$$

The second objective function is included so that the vibration of the flexible mode can be reduced. In general, the flexural motion is dominated by the first structural mode. Therefore, the tip deflection of the appendage dominates the whole spatial motion for the rest-to-rest maneuver. Especially, the potential energy vanishes at this point by the geometric boundary condition $\partial^2 w(x,t)/\partial x^2 = 0$. Therefore, we can conclude that the vibratory motion of the flexible appendages can be represented by the kinetic energy at the tip of the appendage, and thereby the second objective function is chosen as follows:

$$J_2 = q_m \int_{t_0}^{t_f} \rho \dot{w}^2(l, t) \,\mathrm{d}t \tag{46}$$

where q_θ and q_m are weighting factors for the slewing and vibration energy.

Combined with the time-domain finite element modeling method, the first objective function can be converted as follows:

$$J_1 = q_\theta \int_{t_0}^{t_f} \left\{ \theta(t)^2 - 2\theta(t)\theta_f + \theta_f^2 \right\} \mathrm{d}t = q_\theta \left\{ \frac{\boldsymbol{\theta}^T K\boldsymbol{\theta}}{EI} - 2M_1\boldsymbol{\theta} + \theta_f^2 t_f \right\} \tag{47}$$

where

$$[M_1]_i = \int_{\Delta t} \theta_f \phi_i \,\mathrm{d}t$$

Similarly, the second objective function can be represented using the tip motion of the flexible mode

$$J_2 = q_m \boldsymbol{w}^T(l) M \boldsymbol{w}(l) \tag{48}$$

Let us define the performance index as

$$J = \sum_{i=1}^{2} J_i \tag{49}$$

or it can be expressed in terms of $\boldsymbol{\theta}_a$ as follows:

$$J = \boldsymbol{\theta}_a^T T_{aa} \boldsymbol{\theta}_a - 2q_\theta F_a^T \boldsymbol{\theta}_a + q_\theta \theta_f^2 \boldsymbol{t}_f \tag{50}$$

where

$$T_{aa} = \begin{bmatrix} q_\theta(K/EI) + q_m T_{\theta y}^T \Lambda_a T_{\theta y} & \mathbf{0} & \mathbf{0} \\ \mathbf{0}^T & 0 & 0 \\ \mathbf{0}^T & 0 & 0 \end{bmatrix}$$

$$F_a = \begin{bmatrix} F_r \\ 0 \\ 0 \end{bmatrix}, \qquad \Lambda_a = \begin{pmatrix} \Lambda_\eta & \mathbf{0} \\ \mathbf{0} & \mathbf{0} \end{pmatrix} \tag{51}$$

The feedback gains can be obtained through the optimization procedure with the preceding augmented performance index. The analytic gradients of the performance index used in the optimization are summarized in the Appendix. The optimized control gains depend on the final target angle. There are many space applications where the fixed target angle is assumed, and the proposed optimization scheme can be used for a variety of slew maneuvers.

V. Numerical Results

In this section, several numerical results are provided to verify the parameter optimization method developed in Secs. III and IV. Major configuration parameters of the flexible space structure model are listed in Table 1, and the parameters for the time-domain finite element analysis are summarized in Table 2. Dynamic analyses are performed using the one-fifth reduced-order time finite element model (FEM) to show the effect of substantial model reduction in time.

Figures 1 and 2 show the results for the closed-loop response using the constant gain feedback control law. The term conventional FEM means the space-discretized finite element modeling. In conventional FEM, we used the space-discretized FEM to obtain the matrix differential equation with respect to the generalized coordinates, $M\ddot{\boldsymbol{q}} + K\boldsymbol{q} = Fu$, where the matrices M and K are obtained using the spatial discretization of the flexible appendages. After that, the time response is obtained by using a simple numerical integration with the selected gain set.

The selected feedback gains are $g_1 = 116$, $g_2 = 23$, and $g_3 = 97$, respectively. A relatively large number of finite elements ($n = 133$) is used to simulate the system, because the time response of the system reflects a lot of fluctuation at the transient stage. This requires dense time points and many time modes to represent the response well. Figures 3 and 4 show the results for the closed-loop system

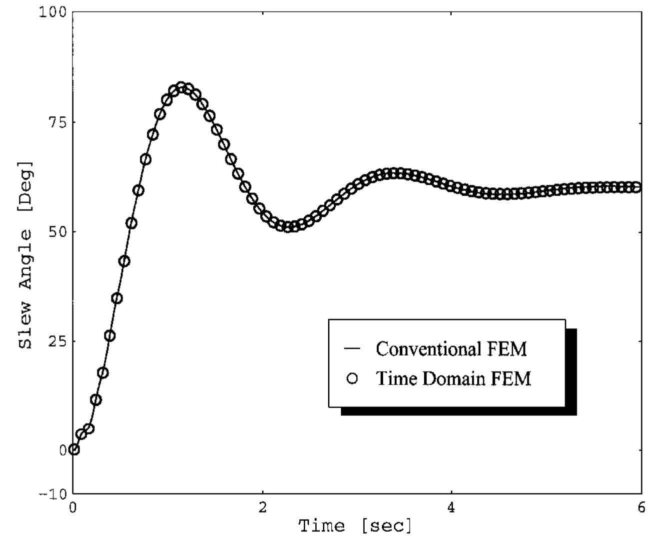

Fig. 1 Slew angle (constant gain control).

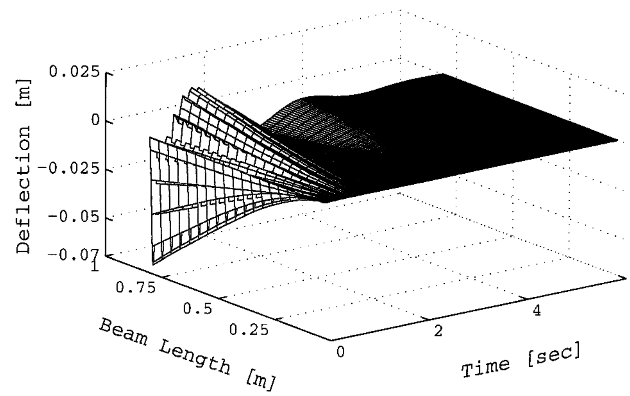

Using conventional FEM

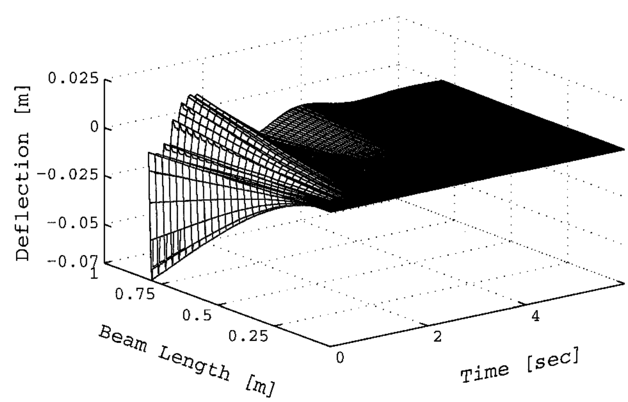

Using time-domain FEM

Fig. 2 Three-dimensional plot for constant gain control.

response using the tracking control law. Open-loop control input is used to derive the reference maneuver. The reference maneuver results from the torque shaping using the Fourier series optimization with the coefficients of the series expansion.[24] Note that the rest-to-rest maneuver guarantees zero initial displacement for both slew and flexible modes. Because the adopted control law is obtained based on the Lyapunov stability theory, a wide range of the gain set can be picked up to constitute a stabilizing tracking control system. The gain set is selected to simulate the dynamic response of the system as $g_1 = 500$, $g_2 = 30$, and $g_3 = 3$, respectively. It is seen from Figs. 3 and 4 that the dynamic motion of the system can be accurately described with only a few time modes ($n = 40$).

Figure 5 shows the performance of the tracking control law with the proposed optimization method that minimizes the selected

Table 1 Configuration parameters for the flexible space structure

Parameter	Value
Radius of hub	0.2000 m
Hub moment of inertia	1.2732 kg · m^2
Density of appendage	2800 kg/m^3
Young's modulus of appendage	7.5842×10^{10} N/m^2
Thickness of appendage	0.0020 m
Width of appendage	0.0635 m
Length of appendage	0.8100 m

Table 2 Parameters for optimization

Gain	$q_\theta = 1, q_m = 5$	$q_\theta = 5, q_m = 5$	$q_\theta = 25, q_m = 5$
g_1	76.2073	104.2416	182.1862
g_2	37.6502	35.9076	40.4663
g_3	63.4303	34.2117	23.7496

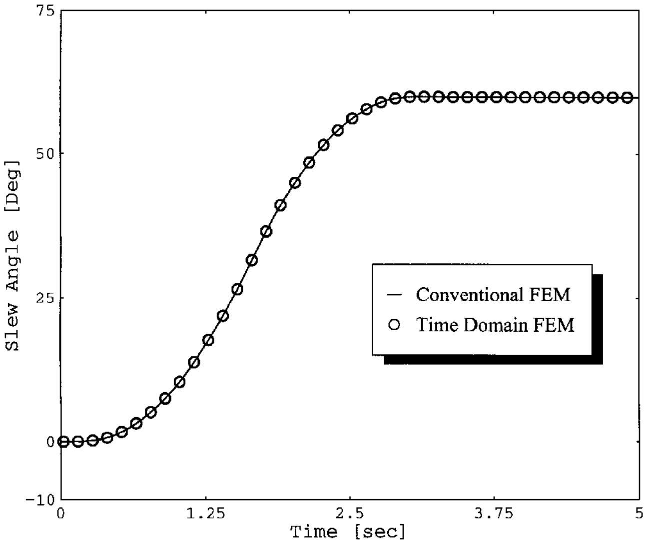

Fig. 3 Slew angle (tracking control).

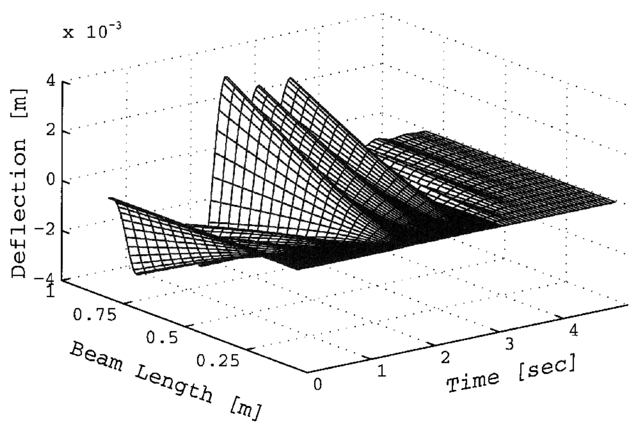

Using conventional FEM

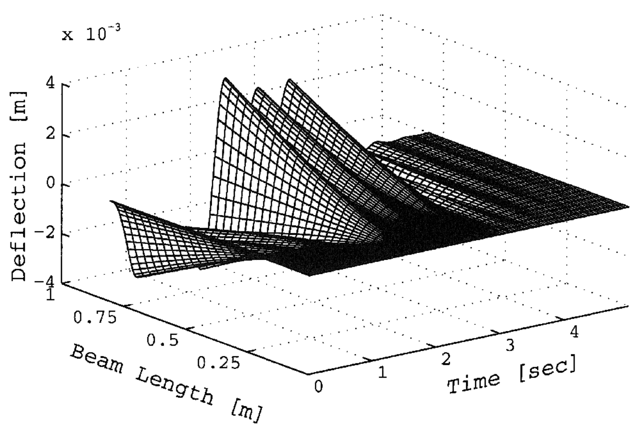

Using time-domain FEM

Fig. 4 Three-dimensional plot for tracking control.

performance index. Weighting factors are chosen so that each objective function may have the same order of value: $q_\theta = 1$ and $q_m = 5$. Compared with the nonoptimized results, the optimized results show better performance in both slewing and vibration control, especially in the latter case, smoothing the high-frequency regions of the vibratory mode and gaining high damping ratio. Figure 6 shows the optimized slewing and vibration suppression performance of the structure with various weightings between the individual control objectives. The results of heavy weighting, q_θ, on slew performance show rapid maneuvers to the target angle while degrading the vibration characteristics of the appendage.

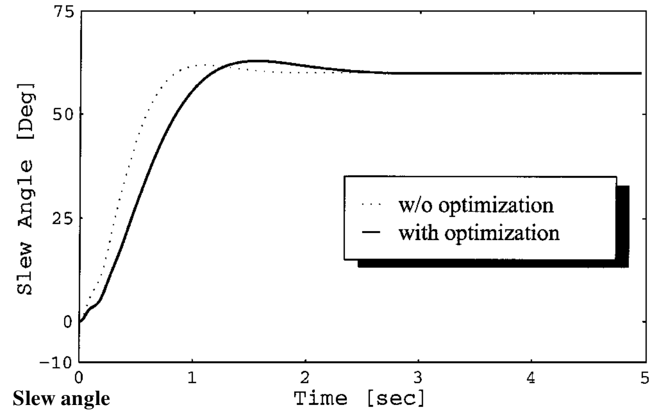

Slew angle

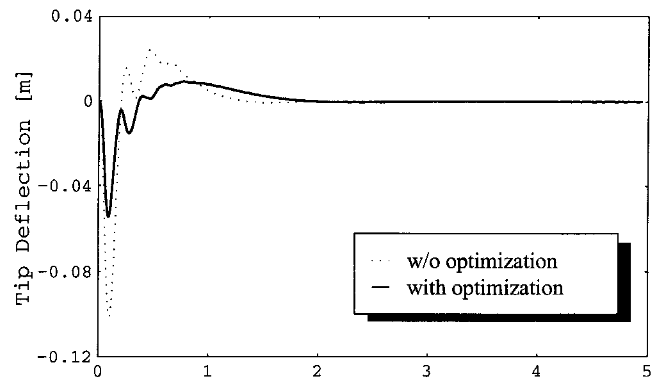

Tip deflection

Fig. 5 Comparative results for optimization.

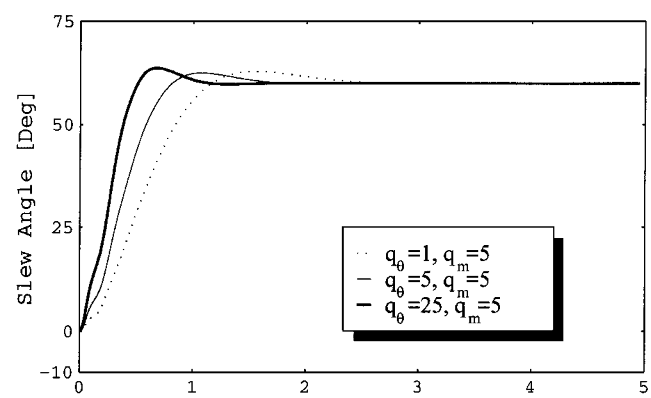

Slew angle

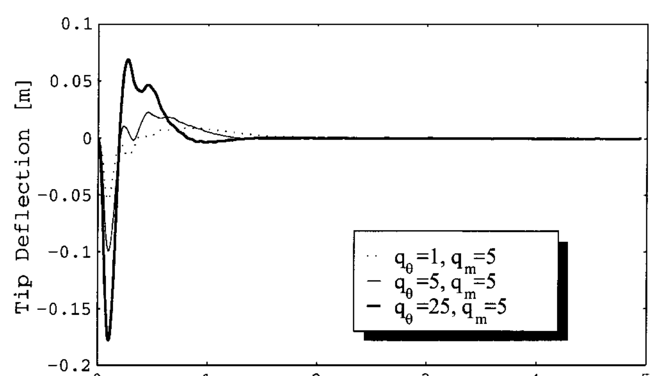

Tip deflection

Fig. 6 Optimized results for various weightings.

VI. Conclusions

This paper presents a design method adopting the Lyapunov control theory combined with time-domain finite element analysis. Two types of Lyapunov control laws are investigated. They are based on the open-loop dynamics in the slew maneuver of flexible space structures. Optimization of the feedback gains is shown as a cogent application for the partial state feedback system. Once the system dynamics is modeled using the time-domain FEM, the ensuing optimization is scheduled by a step-by-step method using a systematic way of constructing the performance index and its derivatives with respect to the design variables in terms of the time-domain state vector. A general performance index based on the energy concept can be obtained easily by using time FEM. Also, the derivatives of the performance index can be expressed analytically for more accurate and efficient optimization. The gradient information with respect to each feedback gain has a much simpler form compared with that given by the conventional eigenvalue analysis. The optimization procedure applied to the slewing of the flexible space structure can be done systematically without violating the time-based model reduction structure of the time-domain FEM. The model reduction technique has already been verified useful as a time saving and accurate method in this particular modeling technique.

Appendix: Analytic Expressions of the Gradients

Analytic gradients of the performance index shown in Sec. IV can be obtained as follows:

$$\frac{\mathrm{d}J}{\mathrm{d}g_j} = 2\left(\frac{\mathrm{d}\boldsymbol{\theta}_a}{\mathrm{d}g_j}\right)^T T_{aa}\boldsymbol{\theta}_a - 2\left(\frac{\mathrm{d}\boldsymbol{\theta}_a}{\mathrm{d}g_j}\right)^T F_a \tag{A1}$$

Detailed derivatives of the individual terms in Eq. (A1) with respect to each gain are

$$\frac{\mathrm{d}\boldsymbol{\theta}_a}{\mathrm{d}g_j} = T_a^{-1}\left\{\frac{\mathrm{d}F_a}{\mathrm{d}g_j} - \frac{\mathrm{d}T_a}{\mathrm{d}g_j}\boldsymbol{\theta}_a\right\} \tag{A2}$$

$$\frac{\mathrm{d}F_a}{\mathrm{d}g_1} = \begin{bmatrix} 2T_0^T F_r + 2g_1(K/EI)F_r \\ 0 \\ 0 \end{bmatrix}, \qquad \frac{\mathrm{d}F_a}{\mathrm{d}g_2} = \begin{bmatrix} 2g_1 C^T F_r \\ 0 \\ 0 \end{bmatrix}$$

$$\frac{\mathrm{d}F_a}{\mathrm{d}g_3} = \begin{bmatrix} -2g_1\{[(l^3 - r^3)/3]M + X^T M\}F_r \\ 0 \\ 0 \end{bmatrix} \tag{A3}$$

$$\frac{\mathrm{d}T_a}{\mathrm{d}g_j} = \begin{bmatrix} 2\frac{\mathrm{d}}{\mathrm{d}g_j}\left(T_0^T T_0\right) & \mathbf{0} & \mathbf{0} \\ \mathbf{0}^T & 0 & 0 \\ \mathbf{0}^T & 0 & 0 \end{bmatrix} \tag{A4}$$

$$\frac{\mathrm{d}}{\mathrm{d}g_1}\left(T_0^T T_0\right) = \frac{K}{EI}T_0 + T_0^T\frac{K}{EI} \tag{A5}$$

$$\frac{\mathrm{d}}{\mathrm{d}g_2}\left(T_0^T T_0\right) = C^T T_0 + T_0^T C \tag{A6}$$

$$\frac{\mathrm{d}}{\mathrm{d}g_3}\left(T_0^T T_0\right) = -\left(\frac{l^3 - r^3}{\rho}M + X^T M\right)T_0 - T_0^T\left(\frac{l^3 - r^3}{\rho}M + X^T M\right) \tag{A7}$$

where $X = P_\eta\{\Pi_{11,44} - \Gamma_{11,34}\Omega_{22}^{-1}\Psi_{34,44}\}P_\eta^T M$.

Acknowledgment

This research was supported in part by a grant from the BK-21 Program for Mechanical and Aerospace Engineering Research at Seoul National University.

References

[1]Bailey, C. D., "Application of Hamilton's Law of Varying Action," *AIAA Journal*, Vol. 13, No. 9, 1975, pp. 1154–1157.

[2]Bailey, C. D., "Direct Analytical Solutions to Non-Uniform Beam Problems," *Journal of Sound and Vibration*, Vol. 56, No. 4, 1978, pp. 501–507.

[3]Simkins, T. E., "Unconstrained Variational Statements for Initial and Boundary-Value Problems," *AIAA Journal*, Vol. 16, No. 6, 1978, pp. 559–563.

[4]Hodges, D. H., and Hou, L. J., "Shape Functions for Mixed p-Version Finite Elements in the Time Domain," *Journal of Sound and Vibration*, Vol. 145, No. 2, 1991, pp. 169–178.

[5]Borri, M., Ghiringhelli, G., Lanz, M., Mantegazza, P., and Merlini, T., "Dynamic Response of Mechanical Systems by a Weak Hamiltonian Formulation," *Computers and Structures*, Vol. 20, No. 1–3, 1985, pp. 495–508.

[6]Öz, H., and Adiguzel, E., "Hamilton's Law of Varying Action, Part I: Assumed-Time-Modes Method," *Journal of Sound and Vibration*, Vol. 179, No. 4, 1995, pp. 697–710.

[7]Hodges, D. W., and Bless, R. R., "Weak Hamiltonian Finite Element Method for Optimal Control Problems," *Journal of Guidance, Control, and Dynamics*, Vol. 14, No. 1, 1991, pp. 148–156.

[8]Bless, R. R, Hodges, D. H., and Seyward, H., "Finite Element Method for the Solution of State-Constrained Optimal Control Problems," *Journal of Guidance, Control, and Dynamics*, Vol. 18, No. 5, 1995, pp. 1036–1043.

[9]Hodges, D. H., Bless, R. R., Calise, A. J., and Leung, M., "Finite Element Method for Optimal Guidance of an Advanced Launch Vehicle," *Journal of Guidance, Control, and Dynamics*, Vol. 15, No. 3, 1992, pp. 664–671.

[10]Lee, S., and Kim, Y., "Time-Domain Finite Element Method for Inverse Problem of Aircraft Maneuvers," *Journal of Guidance, Control, and Dynamics*, Vol. 20, No. 1, 1997, pp. 97–103.

[11]Öz, H., and Adiguzel, E., "Hamilton's Law of Varying Action, Part II: Direct Optimal Control of Linear Systems," *Journal of Sound and Vibration*, Vol. 179, No. 4, 1995, pp. 711–724.

[12]Anderson, B. D. O., and Moore, J. B., *Optimal Control: Linear Quadratic Methods*, Prentice–Hall, Englewood Cliffs, NJ, 1989, Chap. 13.

[13]Kwakernaak, H., and Sivan, R., *Linear Optimal Control Systems*, Wiley, New York, 1972, pp. 377–438.

[14]Bryson, A. E., and Ho, Y. C., *Applied Optimal Control*, Wiley, New York, 1975, pp. 42–89.

[15]Bang, H., Junkins, J. L., and Fleming, P., "Lyapunov Optimal Control Laws for Flexible Structure Maneuver and Vibration Control," *Journal of Astronautical Sciences*, Vol. 41, No. 1, 1993, pp. 91–118.

[16]Kim, Y., Suk, J., Kim, S., and Junkins, J. L., "Near-Minimum-Time Control of Smart Structures for Slew Maneuver," *Journal of Astronautical Sciences*, Vol. 45, No. 1, 1997, pp. 91–111.

[17]Turner, J. D., and Chun, H. M., "Optimal Distributed Control of a Flexible Spacecraft During a Large-Angle Maneuver," *Journal of Guidance, Control, and Dynamics*, Vol. 7, No. 3, 1984, pp. 257–264.

[18]Banerjee, A. K., "Dynamics and Control of WISP Shuttle Antennae System," *Journal of Astronautical Sciences*, Vol. 41, No. 1, 1993, pp. 73–90.

[19]Singhose, W. E., Banerjee, A. K., and Seering, W. P., "Slewing Flexible Spacecraft with Deflection-Limiting Input Shaping," *Journal of Guidance, Control, and Dynamics*, Vol. 20, No. 2, 1997, pp. 291–298.

[20]Suk, J., and Kim, Y., "Slew Maneuver of Flexible Space Structures Using Time Finite Element Analysis," *AIAA Journal*, Vol. 36, No. 10, 1998, pp. 1938–1940.

[21]Suk, J., and Kim, Y., "Time-Domain Finite Element Analysis of Dynamic Systems," *AIAA Journal*, Vol. 36, No. 7, 1998, pp. 1312–1319.

[22]Junkins, J. L., Rahman, Z. H., and Bang, H., "Near-Minimum-Time Control of Distributed Parameter Systems: Analytical and Experimental Results," *Journal of Guidance, Control, and Dynamics*, Vol. 14, No. 2, 1991, pp. 406–415.

[23]Bailey, T., and Hubbard, J. E., "Distributed Piezoelectric-Polymer Active Vibration Control of a Cantilever Beam," *Journal of Guidance, Control, and Dynamics*, Vol. 8, No. 5, 1985, pp. 605–611.

[24]Suk, J., Moon, J. Y., and Kim, Y., "Torque Shaping Using Trigonometric Series Expansion for Slewing of Flexible Structures," *Journal of Guidance, Control, and Dynamics*, Vol. 21, No. 5, 1998, pp. 698–703.

[25]Suk, J., Kim, Y., and Bang, H., "Experimental Evaluation of the Torque Shaping Method for Slew Maneuver of Flexible Space Structures," *Journal of Guidance, Control, and Dynamics*, Vol. 21, No. 6, 1998, pp. 817–822.